Published as: *Cell Rep*. 2013 December 26; 5(6): 1679–1689.

Dynamic Chromatin Modification Sustains Epithelial-Mesenchymal Transition following Inducible Expression of Snail-1

Sarah Javaid[1,7], **Jianmin Zhang**[1,3,6,7], **Endre Anderssen**[1], **Josh C. Black**[1], **Ben S. Wittner**[1], **Ken Tajima**[1], **David T. Ting**[1], **Gromoslaw A. Smolen**[1,4], **Matthew Zubrowski**[1,5], **Rushil Desai**[1], **Shyamala Maheswaran**[1], **Sridhar Ramaswamy**[1], **Johnathan R. Whetstine**[1], and **Daniel A. Haber**[1,2,*]

[1]Massachusetts General Hospital Cancer Center and Harvard Medical School, Charlestown, MA 02129, USA

[2]Howard Hughes Medical Institute, Chevy Chase, MD 20815, USA

SUMMARY

Epithelial-mesenchymal transition (EMT) is thought to contribute to cancer metastasis, but its underlying mechanisms are not well understood. To define early steps in this cellular transformation, we analyzed human mammary epithelial cells with tightly regulated expression of Snail-1, a master regulator of EMT. After Snail-1 induction, epithelial markers were repressed within 6 hr, and mesenchymal genes were induced at 24 hr. Snail-1 binding to its target promoters was transient (6–48 hr) despite continued protein expression, and it was followed by both transient and long-lasting chromatin changes. Pharmacological inhibition of selected histone acetylation and demethylation pathways suppressed the induction as well as the maintenance of Snail-1-mediated EMT. Thus, EMT involves an epigenetic switch that may be prevented or reversed with the use of small-molecule inhibitors of chromatin modifiers.

INTRODUCTION

The ability of cells to cycle between epithelial and mesenchymal states is critical for normal development. While mesenchymal-to-epithelial transition (MET) is required for renal

*Correspondence: haber@helix.mgh.harvard.edu.
[3]Present address: Roswell Park Memorial Cancer Institute, Buffalo, NY 14263, USA
[4]Present address: Agios Pharmaceuticals, Cambridge, MA 02139, USA
[5]Present address: Novartis Institutes for BioMedical Research, Cambridge, MA 02139, USA
[6]Present address: The First Affiliated Hospital of Xi'an Jiaotong University, 710061 Shaanxi, China
[7]These authors contributed equally to this work

ACCESSION NUMBERS

The NCBI Gene Expression Omnibus accession number for the data reported in this paper is GSE52593.

SUPPLEMENTAL INFORMATION

Supplemental Information includes six figures and nine tables and can be found with this article online at http://dx.doi.org/10.1016/j.celrep.2013.11.034.

epithelial differentiation in response to signals from the ureteric bud, epithelial-to-mesenchymal transition (EMT) is essential for the development of melanocytes, heart valves, and neural-crest-derived tissues (Thiery et al., 2009). The aberrant acquisition by epithelial cells of mesenchymal features, including loss of apico-basal polarity, increased migratory potential, and resistance to apoptotic stimuli, has been implicated in models of cancer invasion and metastasis (Nieto, 2011). Moreover, shared characteristics between cells subjected to EMT and stem or progenitor cell populations have raised the possibility that both involve fundamental properties involved in cell differentiation and regenerative potential (Mani et al., 2008).

Despite the dramatic changes associated with EMT, the mechanisms underlying this phenomenon are only partially understood. In nontransformed epithelial cells, prolonged (7 days) exposure to transforming growth factor β (TGF-β) is required to trigger loss of epithelial markers, such as E-cadherin and EpCAM, and induce expression of mesenchymal markers, including Vimentin and N-cadherin (Leivonen and Kähäri, 2007). Additional growth factors implicated in triggering EMT include epidermal growth factor, hepatocyte growth factor, platelet-derived growth factor, insulin growth factor, and Wnt (Scheel and Weinberg, 2011, Thiery and Sleeman, 2006, Yang and Weinberg, 2008). Downstream of these signaling molecules are a set of transcriptional regulators, including Twist, Snail-1, Slug, Zeb1, and Sip1 (Peinado et al., 2007), whose expression is sufficient to induce EMT in epithelial cells. We recently identified a developmentally regulated transcription factor, LBX1, that itself regulates TGF-β2, Snail-1, Zeb1, and Sip1 (Yu et al., 2009). MicroRNAs, namely, the miR-200 family and miR-205, have been shown to regulate EMT by targeting Zeb1 and Sip1 (Gregory et al., 2008, Korpal and Kang, 2008). Thus, the induction and maintenance of EMT may involve the coordination of multiple regulatory components whose integration is key for this profound change in cell fate.

A number of distinct mechanisms may underlie the integration of complex cellular signals resulting in EMT. Scheel et al. (2011) proposed that autocrine BMP and Wnt signaling may establish self-sustaining feedback loops that are sufficient to induce and maintain the EMT state. Suppression of the epithelial marker E-cadherin is itself capable of triggering EMT, suggesting another feedback pathway involving the loss of cell-surface-mediated signaling (Onder et al., 2008). Alternatively, EMT may result from a global chromatin switch, analogous to other cell-fate changes that arise during physiological development. Indeed, global chromatin modifications have been noted under specific conditions, such as hypoxia-induced EMT in the FADU epithelial cell line or TGF-β-induced EMT in mouse hepatocytes (McDonald et al., 2011, Wu et al., 2011). Given the presumed role of EMT in cancer progression, defining the mechanisms that sustain this phenotype in cancer cells may provide important therapeutic opportunities.

Snail family members encode zinc-finger-type transcription factors that induce EMT during mesoderm and neural crest formation (Blanco et al., 2002). The prototype Snail-1 mediates transcriptional repression of E-cadherin and other epithelial markers, such as claudins, cytokeratins, mucins, plakophilin, occludin, and ZO proteins (Batlle et al., 2000, Cano et al., 2000, Thiery et al., 2009), binding to E-box consensus sequences and recruiting chromatin modifiers, including SIN3A, histone deacetylase 1 (HDAC1), HDAC2, lysine-specific

demethylase 1 (LSD1), and components of the Polycomb-2 complex (Herranz et al., 2008, Peinado et al., 2004). Here, we used tightly regulated inducible expression of Snail-1 to trigger EMT and measure the temporal pattern of immediate transcriptional and chromatin changes. We find that Snail-1 binds transiently to its target promoters, triggering transient and long-lasting chromatin changes that appear to underlie EMT. Small-molecule inhibitors of HDACs and LSD1/LSD2 suppress Snail-1-induced EMT and may point the way toward pharmacological approaches to reverse EMT in cancer.

RESULTS

Inducible Snail-1 Induction Leads to EMT

To generate a potent reversible EMT-inducing stimulus, we created a Snail-1 retroviral expression construct using a fused estrogen receptor (ER) response element to mediate regulation by exogenous 4-hydroxy-tamoxifen (4-OHT). Since Snail-1 protein stability and nuclear localization are suppressed by GSK3-β-mediated phosphorylation, we substituted the six targeted amino acids (ER-Snail-1^{6SA}), thus conferring constitutive activity to the induced protein (Zhou et al., 2004). Infection of nontransformed, immortalized human mammary epithelial MCF10A cells with ER-Snail-1^{6SA}, followed by treatment with 4-OHT, triggered morphological and biomarker characteristics of EMT (Figures 1A and 1B). A similar phenotype was induced in MCF7 human breast adenocarcinoma cells (Figure S1A), and no such effect was observed using the retroviral construct in the absence of 4-OHT (data not shown), or by 4-OHT alone in noninfected cells (Figure S1B). In contrast to most model systems, which involve prolonged exposure to TGF-β or ectopic Snail-1, the rapid induction of EMT made it possible to dissect the relative timing of key characteristics, including increased cell migration, loss of epithelial markers, and induction of mesenchymal markers.

As expected, Snail-1 induction resulted in loss of epithelial markers (i.e., CDH1 and CDH3) and gain of mesenchymal markers (i.e., FN1 and SERPINE1), detected at both RNA and protein levels (Figures 1B–1E). Epithelial gene repression was evident as early as 6 hr after 4-OHT treatment, whereas induction of mesenchymal transcripts did not start until 24 hr after Snail-1 activation (Figures 1D and 1E). A comparable, albeit delayed, time course of epithelial gene repression and mesenchymal gene induction was evident in EMT induced by TGF-β (Figures S1C and S1D). Increased cell migration, a key EMT-associated phenotype linked to cancer metastasis, was virtually immediate following Snail-1 induction. Indeed, by measuring real-time cell migration, we observed increased migration of MCF10A cells as early as 4 hr following 4-OHT treatment, with a continuous rise in cell motility accompanying continued Snail-1 induction (Figures 1F and S1E). Decreased cell proliferation, another phenotype associated with EMT (Vega et al., 2004), was evident as early as 24 hr (Figure S1F).

Dynamic Patterns of Gene Expression Associated with Induction of EMT

The acute initiation of EMT by inducible Snail-1 made it possible to identify a timeline of transcriptional changes that are integral to this cellular transformation. Microarray-based expression profiling combined with principal component analysis (PCA) revealed a time-dependent connectivity pattern as cells progressed from epithelial to mesenchymal states

(Figure 2A). Early time points (3, 6, and 12 hr) were clustered together, marking the immediate response to Snail-1. Thereafter, cells progressed toward an intermediate state (24 and 72 hr) and a fully mesenchymal state (120 hr; Figure 2A).

We identified six distinct classes of Snail-1-dependent transcripts: cluster I, transcripts repressed early (<24 hr, n = 712 transcripts); cluster II, transcripts repressed late (>24 hr, n = 503); cluster III, transiently repressed transcripts (between 6 and 72 hr, n = 24); cluster IV, transcripts induced early (<24 hr, n = 363); cluster V, transcripts induced late (>24 hr, n = 1716); and cluster VI, transiently induced transcripts (between 6 and 72 hr, n = 64; Figure 2B; Tables S1–S6). Characteristic epithelial markers, such as CDH1 and OCLDN, were suppressed early (cluster I). Although less immediate in their Snail-1-driven induction, characteristic mesenchymal markers, including FN1 and CTGF, were among the early-induced transcripts (cluster IV; Figures 1 and 2B).

By Gene Set Enrichment Analysis (GSEA), with a false discovery rate (FDR) threshold of 0.25, most clusters were found to be enriched for signatures of breast cancer-associated genes (Tables S1–S6) and genes implicated in EMT, extracellular matrix (ECM), metastasis, and cell migration (Figure 2C; Tables S1–S6). GSEA of transcripts repressed early, late, or transiently (clusters I–III) included gene sets associated with the repressive histone mark H3K27Me3, genes downregulated in cell lines resistant to therapeutic drugs, as well as gene targets of microRNAs (as many as 20% of genes in clusters I and II; Figure 2C; Tables S1–S6). Conversely, transcripts induced early, late or transiently (clusters IV–VI) were enriched in GSEA gene sets associated with cell migration, and in genes whose expression is downregulated in response to HDAC1, HDAC2, and HDAC3 knockdown (Figure 2C; Tables S1–S6). Both induced and repressed gene clusters included large numbers of transcriptional regulators (14% of genes in cluster II, and 1%–6% of genes in clusters I and III–VI), consistent with the presumed role of Snail-1 as a master transcriptional regulator (Table S7). Thus, EMT initiation involves the upregulation and downregulation of distinct functional groups and pathways.

Transient Promoter Binding by Snail-1 during Induction of EMT

The complex transcriptional patterns associated with induction of Snail-1 expression may result from direct Snail-1 promoter binding as well as secondary effects mediated by downstream transcription factors. To define the time-dependent binding of Snail-1 to its target promoters following its activation by 4-OHT, we first studied the prototypical CDH1 (epithelial) and Vimentin (mesenchymal) promoters (time points: 0, 3, 6, 24, 48, 72, and 120 hr). Remarkably, Snail-1 binding to the CDH1 promoter was transient, despite continued Snail-1 protein expression. Snail-1 binding was evident by 3 hr postinduction (p value % 0.001 compared with time point 0 hr) and it disappeared by 48 hr (Figure 3A). In contrast, no incremental change in Snail-1 binding was evident at the Vimentin promoter, suggesting that its activation may be the indirect consequence of transcriptional intermediates (Figure 3A).

We next applied genome-wide chromatin immunoprecipitation (ChIP)-chip analyses to extend the Snail-1-binding studies to a broad set of target promoters at multiple time points following Snail-1 induction (time points: 0, 6, 48, and 120 hr). By analyzing paired ChIP-

chip measurements with matched microarrayed expression clusters, we found that Snail-1 binding was evident in proximal promoter regions (−2 kb to +2 kb with respect to the transcriptional start site [TSS]) between 6 to 48 hr, with loss of Snail-1 enrichment at 120 hr (Figures 3B and S2A). This transient Snail-1 enrichment was observed for 60% of early-repressed genes (cluster I) and 45% of late-repressed genes (cluster II; Figure 3B; Table S8). Surprisingly, given Snail-1's presumed function as a transcriptional repressor, Snail-1 binding was also observed for up to 39% of early-induced gene promoters (cluster IV; peak binding 48 hr) and up to 32% of transiently induced transcripts (cluster VI; Figure 3B; Table S8). In contrast, late-induced genes (cluster V) did not show significant enrichment for Snail-1 binding, consistent with indirect transcriptional regulation.

To confirm that transient binding of Snail-1 to its target promoters is correlated with their respective gene expression, transcripts in all clusters (I–VI) were binned according to expression level and plotted against the density of promoter-bound Snail-1 at 6 hr (enrichment for Snail-1) and 120 hr (loss of Snail-1 enrichment). Early- and late-repressed clusters (clusters I and II) revealed a linear relationship between the logarithm of expression and density of Snail-1 binding at 6 hr (Figure 3C). No such relationship was detected at 120 hr, when Snail-1 promoter binding is no longer enriched (Figure S2B). Early- and transiently induced genes (clusters IV and VI) also revealed a linear relationship between target gene expression and Snail-1 promoter binding density (Figures 3C and S2B). Together, these observations suggest that a relatively brief promoter occupancy by Snail-1 is sufficient to trigger long-term transcriptional changes associated with a sustained mesenchymal phenotype. In addition, a subset of induced genes show direct promoter binding by Snail-1, suggesting that it can function as an activator, as well as a repressor, of its direct target genes.

Sustained Chromatin Marks at Snail-1-Regulated Promoters

To test whether Snail-1 binding is associated with time-dependent chromatin modifications, we measured $\log_2$ ratio changes in the chromatin marks H3K4Me1, H3K4Me2, H3K4Me3, H3K27Me3, H3K4Ac, and H3K27Ac, all within −2 kb to +2 kb of the TSS for Snail-1 regulated transcripts (Figures S3A–S3F and S4A–S4F). Multiple time points (0, 6, 48, and 120 hr) following Snail-1 induction were assayed using ChIP-chip and confirmed using ChIP-quantitative PCR (ChIP-qPCR) experiments for selected targets (CDH1 and VIM; Figures S3A–S3F). Given the dynamic nature of gene-expression changes observed during the initiation of EMT, we grouped the histone modifications within each expression cluster (I–VI). Genes that are rapidly silenced upon EMT initiation (cluster I) showed a loss of active marks (H3K4Ac, H3K27Ac, and H3K4Me3) while gaining the repressive H3K27Me3 modification. Enrichment of H3K4Me1 was observed gradually over the course of EMT (Figure 4A). Genes that were silenced >24 hr after induction of Snail-1 (cluster II) showed a similar loss of active marks (H3K4Ac and H3K4Me3) and gain of the repressive mark H3K27Me3 (Figure 4A). In contrast, transiently repressed genes (cluster III) showed coincident loss of both active H3K4Ac and inactive H3K27Me3 repressive marks, without changes in H3K27Ac and H3K4Me3 (Figure 4A).

Promoters of genes induced early following Snail-1 induction (cluster IV) showed gains of the active H3K4Me3 mark and of H3K4Me1, together with loss of the repressive H3K27Me3 mark (Figure 4B), whereas late-induced genes (cluster V) showed primarily loss of H3K27Me3 (Figure 4B). Chromatin changes for transiently induced genes (cluster VI), including H3K27Ac, H3K27Me3, and H3K4Me3, were themselves transient (Figure 4B). Overall, promoters of Snail-1-induced transcripts showed more heterogeneous chromatin changes compared with promoters of Snail-1-repressed genes, consistent with the former having more indirect and potentially diverse epigenetic mechanisms. Of note, the timeline of both activating and repressive chromatin marks was delayed compared with the initial Snail-1 promoter binding and early transcriptional changes. Thus, direct transcriptional regulation by Snail-1 may precede the deposition of classical chromatin silencing and activating marks that ultimately maintain the mesenchymal state after Snail-1 has been released from its target promoters.

Suppression of Induction and Maintenance of EMT by Small-Molecule Inhibitors of Chromatin Regulators

The apparent role of chromatin modifications in the fixation of EMT raised the possibility that inhibition of selected pathways might be capable of modulating this phenotype. Given the observed correlation between Snail-1-mediated repression and loss of H3K4Ac and H3K27Ac, along with the number of HDAC targets (HDAC1, HDAC2, and HDAC3) among the Snail-1-regulated transcripts, we first tested the effect of individual HDAC gene knockdown (Figures 5A and S5A). siRNA-mediated knockdown of either HDAC1 or HDAC3 reduced mesenchymal gene induction by Snail-1 (Figures 5A and S5A). Knockdown of HDAC2 had no effect on mesenchymal gene induction, and none of the HDAC knockdowns significantly affected epithelial gene repression by Snail-1. A very modest reduction in CDH1-specific suppression by Snail-1 was observed following HDAC1 knockdown, as previously reported (Peinado et al., 2004; Figure 5A).

To extend our studies to the larger family of HDACs and other chromatin modifiers, we turned to class-specific small-molecule inhibitors and tested their effect on both the induction and maintenance of EMT. Cells were initially pretreated for 24 hr with inhibitors, which were then maintained in the culture medium as EMT was induced with 4-OHT for 48 hr. Induction of EMT by Snail-1 was not affected by pretreatment of cells with the DNA methylation inhibitor 5-azacytidine or the SIRTUIN inhibitor nicotinamide (Figures 5B and S5B). However, pretreatment of cells with either the LSD1/LSD2 inhibitor Tranylcypromine (TCP) or the HDAC class I and II inhibitor Trichostatin A (TSA) attenuated both Snail-1-mediated downregulation of epithelial markers and upregulation of mesenchymal markers (Figures 5B, S5B, and S6A). Combined treatment with TCP and TSA completely abrogated EMT (Figures 5B and S5B). To test whether this inhibitory effect on the initiation of Snail-mediated EMT was shared with other triggers of EMT, we tested these inhibitors in cells exposed to TGF-β for 48 hr. Pretreatment of cells with TSA and TCP was even more potent in inhibiting TGF-β-induced EMT marker expression (Figures 5C and S5C). Although the precise specificity of small-molecule inhibitors is not fully characterized, we tested more selective inhibitors, including SAHA (Vorinostat, an HDAC1, HDAC2, HDAC3, and HDAC9 inhibitor), LBH589 (Panobinostat, an HDAC1, HDAC2, HDAC3 and HDAC6

inhibitor), pargyline (an LSD1 inhibitor), Tubastatin A (an HDAC6 and HDAC8 inhibitor), MS-275 (Entinostat, an HDAC1 and HDAC3 inhibitor), and PXD101 (Belinostat, an HDAC inhibitor). Pargyline and LBH589 fully abrogated Snail-1-induced EMT, whereas SAHA selectively abolished mesenchymal gene induction (Figures 5D and S5D). MS-275 and PXD101 had only modest effects on mesenchymal markers, and Tubastatin A was ineffective (Figures 5D and S5D). Thus, although drug-specific differences were apparent, HDAC and LSD1/LSD2 inhibitors can suppress the induction of EMT.

To test whether HDAC inhibitors can reverse established EMT, we induced Snail-1 expression for 6 days and then added chromatin inhibitors for 24 hr. Remarkably, TSA alone mediated almost complete reversion of mesenchymal gene expression while also triggering a modest reversal in epithelial gene repression (Figures 5E and S5E). Similarly, EMT established by 12 days of TGF-β exposure was largely abrogated upon TSA treatment (Figures 5F and S5F). No change in EMT established by Snail-1 or TGF-β was observed following treatment with 5-azacytidine, nicotinamide, or TCP. Together, these observations support an important role for chromatin modifications in both the establishment and maintenance of EMT. Moreover, these results indicate that TCP (an LSD1/LSD2 inhibitor) can attenuate the induction of EMT, whereas HDAC inhibitors (e.g., TSA) can inhibit both the induction and maintenance of EMT.

Having tested the effect of small-molecule inhibitors in a short-term assay of Snail-1- and TGF-β-mediated EMT in nontransformed MCF10A cells, we turned to established human breast cancer cells that had undergone EMT during tumorigenesis. We treated MCF7 and triple-negative (TN; lacking ER, progesterone receptor, and human epidermal growth factor receptor 2 expression) breast cancer cells with mesenchymal (M) features (MDA-MB-231, BT549, and Hs578T) or basal (B) features (MDA-MB-468 and HCC1937) with small-molecule inhibitors (Figures 6A, S6B, and S6C). Three of the five cell lines (MDA-MB-468, BT549, and HCC1937) showed suppression of mesenchymal gene expression following treatment with TSA, MS-275, or LBH589, and the other two (MDA-MB-231 and Hs578T) had a more modest reduction in mesenchymal gene expression (Figures 6A, S6B, and S6C). Almost no change in epithelial gene expression was observed following drug treatment (Figure S6C). Although the magnitude of the changes in EMT markers was not as pronounced as that seen in MCF10A breast epithelial cells acutely exposed to Snail-1 or TGF-β, these observations point to a significant degree of reversibility in mesenchymal cell fate even in established tumor cell lines. Moreover, in three of these five triple-negative breast cancer lines, the reduction in mesenchymal markers was associated with a rapid and profound decline in cellular motility (Figure 6B).

DISCUSSION

We have shown that Snail-1 triggers sustained but reversible epigenetic changes, leading to mesenchymal transformation in nontransformed human breast epithelial cells. Even when induced continuously, Snail-1 binds only transiently (6–48 hr) to its target repressed promoters with loss of activation marks and gain of chromatin silencing marks being detectable after Snail-1 itself is no longer immunoprecipitated from its target promoters. Together, these observations support the concept of EMT induction as an epigenetic switch,

a model that is supported by the effectiveness of HDAC inhibitors in abrogating its induction and maintenance. Given the rapidly expanding number of small-molecule inhibitors, with increasing specificity in targeting individual components of the chromatin remodeling machinery, these studies raise the possibility of ultimately suppressing the mesenchymal phenotype associated with cancer invasion and metastasis.

The role of Snail-1 as a master transcriptional regulator mediating EMT is well established (Batlle et al., 2000, Cano et al., 2000, Herranz et al., 2008, Lin et al., 2010, Peinado et al., 2004) and our analysis provides a comprehensive timeline of transcriptional outputs following Snail-1 activation (Tables S1–S7). Binding of Snail-1 to the promoters of down- or upregulated gene transcripts was evident for many, but not all, targets, pointing to both direct and indirect effects within a cascade of downstream transcriptional effectors. While Snail-1 is thought to function primarily as a transcriptional repressor, we did observe Snail-1 binding to a subset of upregulated gene promoters, raising the possibility that these promoters may be directly transcriptionally activated by Snail-1. Such an effect might reflect promoter context and recruitment of associated cofactors, including HDAC1, HDAC2, and SIN3A. Of note, ChIP-chip studies have suggested that in developing Drosophila embryos, Snail-1 may act as both a transcriptional activator and repressor (Zeitlinger et al., 2007). Given the long-lasting effects of Snail-1 on its transcriptional targets, the fact that it binds to target promoters only transiently was unexpected. The determinants of this transient binding activity are unclear, and could involve the recruitment of additional cofactors that release Snail-1 from its binding site, or alternatively the Snail-1-induced chromatin changes could themselves reduce binding by Snail-1. Similar transient promoter binding characteristics have been described for c-Myc in the context of cellular reprogramming to generate induced pluripotent stem cells, as well as during cell-cycle progression (Brambrink et al., 2008, Sridharan et al., 2009, Swarnalatha et al., 2012).

In this work, we analyzed chromatin changes triggered by Snail-1 in conjunction with early, late, and transient transcriptional changes. We found loss of H3K4Me3, H3K4Ac, and H3K27Ac, and gain of H3K27Me3 for genes repressed during EMT. Among the genes activated by Snail-1, the most consistent pattern was observed for those induced early, which showed gain of H3K4Me3 and H3K4Me1, and loss of H3K27Me3. Such chromatin changes are consistent with a programmed epigenetic switch linked to EMT. Indeed, constitutive expression of Snail-1 in trophoblast stem cells results in global loss of acetylation on histones H2A and H2B (Abell et al., 2011), and hypoxia-induced EMT has been linked to H3K4 deacetylation at epithelial genes and H3K4 methylation at mesenchymal genes (Wu et al., 2011). In addition, TGF-β-mediated EMT appears to reduce H3K9Me2 and increase H3K4Me3 within large heterochromatin domains (LOCKs), with increased H3K36Me3 at LOCK boundaries (McDonald et al., 2011). Building on these observed EMT-associated changes in chromatin, our ability to acutely trigger Snail-1-mediated EMT and correlate promoter chromatin marks with time-dependent global transcriptional patterns thus provides a comprehensive view of the differential changes affecting a broad array of functionally related genes.

Considerable advances have recently been made in the generation of small-molecule inhibitors of chromatin regulators, raising the possibility of targeting chromatin processes

for therapeutic intervention. Although the specificity of these inhibitors remains suboptimal and the physiological properties of their gene targets are incompletely understood, they provide critical tools to probe the functional consequences of disrupting subsets of chromatin modifications. Some of these inhibitors, such as SAHA and Vorinostat, have already been approved to treat cutaneous T cell lymphoma, and other HDAC inhibitors are currently in clinical trials. Given the redundancy of chromatin regulators, small-molecule inhibitors suppress large subsets of these gene families, and our initial analyses will need to be refined as further specific inhibitors become available. Nonetheless, the observed synergy between HDAC and LSD1/LSD2 inhibitors suggests that suppressing the removal of H3K4Me1, H3K4Me2, and histone acetylation marks is sufficient to preserve an active chromatin configuration at key promoters targeted by the Snail-1 transcriptional repressor, thus abrogating EMT. The potent effect of HDAC inhibitors may reflect both derepression of epithelial genes and potentially indirect repression of mesenchymal genes (Jordaan et al., 2013, Mariadason et al., 2000, Gryder et al., 2012, Wagner et al., 2010). In our study, we observed inhibitory effects of TCP and TSA with both Snail-1 and TGF-β-induced EMT, leading to dramatic suppression of both initiation and maintenance of this phenotype. The effect of these small-molecule inhibitors on established cancer cell lines, whose mesenchymal properties emerged during tumorigenesis and were maintained for prolonged periods of time in culture, was more modest but nonetheless remarkable. A significant reduction of tumor cell migration was associated with drug treatment, raising the possibility of modifying such properties in established cancer cells.

In summary, our study lays a foundation for understanding the transcriptional landscape of EMT initiation by a master transcriptional regulator. In addition to providing evidence supporting an epigenetic mechanism for the induction and maintenance of EMT, our analysis points to potential therapeutic approaches to modulate this phenotype, which is implicated in cancer invasion and metastasis.

EXPERIMENTAL PROCEDURES

Tissue Culture and Plasmids

MCF10A cells were cultured as described previously (Debnath et al., 2003). Recombinant human TGF-β1 was obtained from R&D Systems. The human Snail-1 open reading frame with six serine to alanine mutations (Zhou et al., 2004) was fused with modified ER and cloned into the PBABEpuro retroviral expression vector. Retrovirus packaging, MCF10A transduction, and puromycin selection were performed as described previously (Zhang et al., 2008). For real-time migration measurements, AceaE-plates and CIM-plates 16 were used with an xCELLigence system. Following a 1 hr background measurement, cells were seeded (50,000 cells/100 μl well) and the impedance was monitored continually for 24 hr.

Immunoblot Analysis and qRT-PCR Analyses

Cells were harvested in 13 RIPA buffer containing 13 protease inhibitor cocktail (Complete EDTA-free; Roche). Cell lysates were cleared by centrifugation at 14,000 rpm for 10 min at 4°C. For immunoblotting analysis, lysates were loaded onto 4%–15% SDS-PAGE gels (ReadyGel; Bio-Rad) and subsequently transferred onto Immobilon PVDF membrane

(Millipore). Proteins were visualized with the Western Lightning Plus chemiluminescence kit (PerkinElmer). The following antibodies were used: CDH1 (610181; BD Biosciences), CDH3 (610227; BD Biosciences), SERPINE1 (612024; BD Biosciences), FN1 (F3648; Sigma-Aldrich), β-actin (ab6276; Abcam), and Flag (Sigma-Aldrich). For real-time qPCR analyses, RNA was extracted using the RNeasy Mini kit (Qiagen) and cDNA synthesis was performed using SuperScript III reverse transcriptase (Invitrogen). Epithelial and mesenchymal genes were expressed at sufficient levels, thus permitting reliable qPCR quantitation using the Power SYBR Green PCR Master Mix (Applied Biosystems). All samples were done in triplicate and the relative abundance was derived by standardizing the input to the control signal, glyceraldehyde 3-phosphate dehydrogenase. The primer sequences used for qRT-PCR are listed in Table S9.

RNAi Assays and Drug Treatments

A pool of four siRNAs targeting each HDAC1, HDAC2, and HDAC3 was used, along with a nontargeting (control) siRNA from Dharmacon. RNAi transfection was performed according to the manufacturer's protocol. Knockdown of HDAC1, HDAC2, HDAC3, and control were performed 24 hr prior to the addition of 4-OHT. Chemical inhibitor studies for Snail-1 or TGF-β induction experiments were performed by treatment of cells with 50 μMTCP (Sigma-Aldrich) in DMSO, 1 μM TSA (Sigma-Aldrich) in DMSO, 5 μM 5-azacytidine (Sigma-Aldrich) in acetic acid/H_2O (1:1 v/v), 10 mM nicotinamide (Sigma-Aldrich) in H_2O, 1 μM MS-275 (Selleck Chemicals) in DMSO, 1 μM LBH589 (Selleck Chemicals) in DMSO, 1 μM PXD101 (Selleck Chemicals) in DMSO, 1 μM SAHA (Selleck Chemicals) in DMSO, 1 μM Tubastatin A (Selleck Chemicals) in DMSO, and 12.5 μM of Pargyline HCl (Sigma-Aldrich) in H_2O for 24 hr, prior to addition of 4-OHT for another 48 hr. Fresh inhibitor and 4-OHT was added every 24 hr. RNA was extracted, cDNA was synthesized, and qRT-PCR was performed as described above. Paired vehicle controls were performed for each drug target. Chemical inhibitor studies to test the reversibility of Snail-1 or TGF-β-induced EMT were done with the drug concentrations listed above, and the chromatin inhibitors were added for 24 hr, following EMT induction (6 days of Snail-1 induction or 12 days TGF-β pretreatment). The IC_{50} values at 72 hr were as follows: TSA, 6 μM; LBH589, 1.6 μM; MS-275, 11.6 μM; Pargyline HCl, 50.64 μM; and TCP, cannot be determined.

ChIP and Gene Expression Arrays

For RNA expression analysis, RNA was extracted using the RNeasy Mini kit (Qiagen). cDNA synthesis was performed using the Roche cDNA synthesis system (11 117 831 001). cDNA was hybridized to Human Gene Expression 123135K Arrays (Roche Nimblegen) in triplicate according to the manufacturer's protocol. The following antibodies were used for ChIP analyses: Snail-1 (AF3639; R&D Systems), Total H3 (ab1791; Abcam), H3K4Ac (07-539; Millipore), H3K27Ac (ab4729; Abcam), H3K4Me1 (ab8895; Abcam), H3K4Me2 (ab11946; Abcam), H3K4Me3 (ab8580; Abcam), H3K27Me3 (ab6002; Abcam), and immunoglobulin G (IgG; 2729S; Cell Signaling). ChIP was performed as described previously (Black et al., 2010). The primer sequences used for ChIP-qPCR are listed in Table S9. ChIP-chip was performed as described previously (Van Rechem et al., 2011). Snail-1, H3K4Ac, H3K27Ac, H3K4Me1, H3K4Me2, H3K4Me3, and H3K27Me3

immunoprecipitations were amplified with the WGA2 kit (Sigma-Aldrich). The amplified material was hybridized to Human 2.1 M Deluxe HG18 Promoter Arrays (Roche Nimblegen) in duplicates according to the manufacturer's protocol. The microarrays were scanned on a Nimblegen MS200 at 2 μm resolution.

Statistical and Bioinformatic Analyses

All statistical and bioinformatics analyses were performed using R and the Bioconductor software suite. RNA data were preprocessed by the robust multi-array average (RMA) method (Irizarry et al., 2003). ChIP-chip data were preprocessed using the Nimblegen method of the Ringo Bioconductor package (Toedling et al., 2007), quantile normalized, and then smoothed by the application of a 900 bp box filter. Differentially expressed genes (for gene expression or ChIP) were identified for different comparisons using a modified t test (Smyth, 2004) with correction for multiple testing using the method of Benjamini and Hochberg (1995) (p % 0.05 for differential ChIPchip, p % 0.01 for differential gene expression). Hierarchical clustering using correlation distances and the Ward method was performed on the change in gene expression from each respective untreated time point for all genes found to be differentially expressed at the respective treated time point to any subsequent time (3, 6, 12, 24, 72, and 120 hr) for early-, late-, or transiently induced genes, and early-, late-, or transiently repressed genes. Densities were estimated using the density function in R with default parameters. We verified random and known epithelial and mesenchymal genes in clusters I, II, IV, and V. Clusters III and VI were not analyzed. Six out of six genes in cluster I, two out of four genes in cluster II, and five out of five genes in cluster IV were verified. For cluster V, all five genes selected had a delta CT > 35 and were discarded.

GSEA—Enriched gene signatures were manually annotated for their functional categories for each cluster (group and subgroup; for specifics, see Tables S1–S6). For each cluster, the top 100 gene sets were analyzed. If a cluster contained <100 gene sets, all gene sets in that cluster were analyzed. Data are summarized in Figure 2C.

Calculating the Cutoff for Snail-1 Enrichment—For time t and gene g, let $S_{t,g}$ be the average of the $\log_2$ of the Snail-1 ChIP-chip data in a region 2,500 bp on either side of the TSS of the gene. Let $I_{t,g}$ be the same for the input DNA. Let $D_{t,g} = (S_{t,g} - I_{t,g}) - (S_{0,g} - I_{0,g})$. For t = 6, 48, and 120 hr, we plotted an estimate of the density (i.e., the histogram one would get if one had infinitely many data points and infinitely thin bins) of the $D_{t,g}$ for the genes in each of the six clusters.

Determining Genes Enriched for Snail-1—Given that at time 120 hr, the densities of all the clusters are symmetric and centered at zero, we concluded that there is no significant additional binding of Snail-1 at 120 hr compared with 0 hr. Thus, densities at 120 hr were used as a null distribution in the following way: let Y be the 95th percentile of all the $D_{120,g}$. Gene g has significantly more Snail-1 binding at time t than at time 0 if $D_{t,g}$ is greater than Y.

Supplementary Material

Refer to Web version on PubMed Central for supplementary material.

Acknowledgments

We thank Laura Libby for expert technical support and members of the Haber, Maheswaran, Whetstine, and Ramaswamy laboratories for helpful discussions. We thank Nick Dyson for discussions and critical reading of the manuscript. This work was supported by the Howard Hughes Medical Institute (D.A.H.), the NIH (grant CA129933 to D.A.H. and S.J.), Susan G. Komen for the Cure (S.M.), the NCI-MGH Federal Share Program (S.M.), the Ellison Medical Foundation (grants AG-NS-0560-09, CA059267, and R01GM097360 to J.R.W.), and the Jane Coffin Childs Memorial Fund for Medical Research (J.C.B.).

REFERENCES

Abell AN, Jordan NV, Huang W, Prat A, Midland AA, Johnson NL, Granger DA, Mieczkowski PA, Perou CM, Gomez SM, et al. MAP3K4/CBP-regulated H2B acetylation controls epithelial-mesenchymal transition in trophoblast stem cells. Cell Stem Cell. 2011; 8:525–537. [PubMed: 21549327]

Batlle E, Sancho E, Francí C, Domínguez D, Monfar M, Baulida J, García De Herreros A. The transcription factor snail is a repressor of E-cadherin gene expression in epithelial tumour cells. Nat. Cell Biol. 2000; 2:84–89. [PubMed: 10655587]

Benjamini Y, Hochberg Y. Controlling the false discovery rate: a practical and powerful approach to multiple testing. J. R. Stat. Soc. Ser. A Stat. Soc. 1995; 57:289–300.

Black JC, Allen A, Van Rechem C, Forbes E, Longworth M, Tschöp K, Rinehart C, Quiton J, Walsh R, Smallwood A, et al. Conserved antagonism between JMJD2A/KDM4A and HP1g during cell cycle progression. Mol. Cell. 2010; 40:736–748. [PubMed: 21145482]

Blanco MJ, Moreno-Bueno G, Sarrio D, Locascio A, Cano A, Palacios J, Nieto MA. Correlation of Snail expression with histological grade and lymph node status in breast carcinomas. Oncogene. 2002; 21:3241–3246. [PubMed: 12082640]

Brambrink T, Foreman R, Welstead GG, Lengner CJ, Wernig M, Suh H, Jaenisch R. Sequential expression of pluripotency markers during direct reprogramming of mouse somatic cells. Cell Stem Cell. 2008; 2:151–159. [PubMed: 18371436]

Cano A, Pérez-Moreno MA, Rodrigo I, Locascio A, Blanco MJ, del Barrio MG, Portillo F, Nieto MA. The transcription factor snail controls epithelial-mesenchymal transitions by repressing E-cadherin expression. Nat. Cell Biol. 2000; 2:76–83. [PubMed: 10655586]

Debnath J, Muthuswamy SK, Brugge JS. Morphogenesis and oncogenesis of MCF-10A mammary epithelial acini grown in three-dimensional basement membrane cultures. Methods. 2003; 30:256–268. [PubMed: 12798140]

Gregory PA, Bert AG, Paterson EL, Barry SC, Tsykin A, Farshid G, Vadas MA, Khew-Goodall Y, Goodall GJ. The miR-200 family and miR-205 regulate epithelial to mesenchymal transition by targeting ZEB1 and SIP1. Nat. Cell Biol. 2008; 10:593–601. [PubMed: 18376396]

Gryder BE, Sodji QH, Oyelere AK. Targeted cancer therapy: giving histone deacetylase inhibitors all they need to succeed. Future Med. Chem. 2012; 4:505–524. [PubMed: 22416777]

Herranz N, Pasini D, Díaz VM, Francí C, Gutierrez A, Dave N, Escrivà M, Hernandez-Muñoz I, Di Croce L, Helin K, et al. Polycomb complex 2 is required for E-cadherin repression by the Snail1 transcription factor. Mol. Cell. Biol. 2008; 28:4772–4781. [PubMed: 18519590]

Irizarry RA, Hobbs B, Collin F, Beazer-Barclay YD, Antonellis KJ, Scherf U, Speed TP. Exploration, normalization, and summaries of high density oligonucleotide array probe level data. Biostatistics. 2003; 4:249–264. [PubMed: 12925520]

Jordaan G, Liao W, Sharma S. E-cadherin gene re-expression in chronic lymphocytic leukemia cells by HDAC inhibitors. BMC Cancer. 2013; 13:88. [PubMed: 23432814]

Korpal M, Kang Y. The emerging role of miR-200 family of micro-RNAs in epithelial-mesenchymal transition and cancer metastasis. RNA Biol. 2008; 5:115–119. [PubMed: 19182522]

Leivonen SK, Kähäri VM. Transforming growth factor-beta signaling in cancer invasion and metastasis. Int. J. Cancer. 2007; 121:2119–2124. [PubMed: 17849476]

Lin T, Ponn A, Hu X, Law BK, Lu J. Requirement of the histone demethylase LSD1 in Snai1-mediated transcriptional repression during epithelial-mesenchymal transition. Oncogene. 2010; 29:4896–4904. [PubMed: 20562920]

Mani SA, Guo W, Liao MJ, Eaton EN, Ayyanan A, Zhou AY, Brooks M, Reinhard F, Zhang CC, Shipitsin M, et al. The epithelial-mesenchymal transition generates cells with properties of stem cells. Cell. 2008; 133:704–715. [PubMed: 18485877]

Mariadason JM, Corner GA, Augenlicht LH. Genetic reprogramming in pathways of colonic cell maturation induced by short chain fatty acids: comparison with trichostatin A, sulindac, and curcumin and implications for chemoprevention of colon cancer. Cancer Res. 2000; 60:4561–4572. [PubMed: 10969808]

McDonald OG, Wu H, Timp W, Doi A, Feinberg AP. Genome-scale epigenetic reprogramming during epithelial-to-mesenchymal transition. Nat. Struct. Mol. Biol. 2011; 18:867–874. [PubMed: 21725293]

Nie Z, Hu G, Wei G, Cui K, Yamane A, Resch W, Wang R, Green DR, Tessarollo L, Casellas R, et al. c-Myc is a universal amplifier of expressed genes in lymphocytes and embryonic stem cells. Cell. 2012; 151:68–79. [PubMed: 23021216]

Nieto MA. The ins and outs of the epithelial to mesenchymal transition in health and disease. Annu. Rev. Cell Dev. Biol. 2011; 27:347–376. [PubMed: 21740232]

Onder TT, Gupta PB, Mani SA, Yang J, Lander ES, Weinberg RA. Loss of E-cadherin promotes metastasis via multiple downstream transcriptional pathways. Cancer Res. 2008; 68:3645–3654. [PubMed: 18483246]

Peinado H, Ballestar E, Esteller M, Cano A. Snail mediates E-cadherin repression by the recruitment of the Sin3A/histone deacetylase 1 (HDAC1)/HDAC2 complex. Mol. Cell. Biol. 2004; 24:306–319. [PubMed: 14673164]

Peinado H, Olmeda D, Cano A. Snail, Zeb and bHLH factors in tumour progression: an alliance against the epithelial phenotype? Nat. Rev. Cancer. 2007; 7:415–428. [PubMed: 17508028]

Scheel C, Weinberg RA. Phenotypic plasticity and epithelial-mesenchymal transitions in cancer and normal stem cells? Int. J. Cancer. 2011; 129:2310–2314. [PubMed: 21792896]

Scheel C, Eaton EN, Li SH, Chaffer CL, Reinhardt F, Kah KJ, Bell G, Guo W, Rubin J, Richardson AL, Weinberg RA. Paracrine and autocrine signals induce and maintain mesenchymal and stem cell states in the breast. Cell. 2011; 145:926–940. [PubMed: 21663795]

Smyth GK. Linear models and empirical bayes methods for assessing differential expression in microarray experiments. Stat. Appl. Genet. Mol. Biol. 2004; 3 Article3.

Sridharan R, Tchieu J, Mason MJ, Yachechko R, Kuoy E, Horvath S, Zhou Q, Plath K. Role of the murine reprogramming factors in the induction of pluripotency. Cell. 2009; 136:364–377. [PubMed: 19167336]

Swarnalatha M, Singh AK, Kumar V. The epigenetic control of E-box and Myc-dependent chromatin modifications regulate the licensing of lamin B2 origin during cell cycle. Nucleic Acids Res. 2012; 40:9021–9035. [PubMed: 22772991]

Thiery JP, Sleeman JP. Complex networks orchestrate epithelial-mesenchymal transitions. Nat. Rev. Mol. Cell Biol. 2006; 7:131–142. [PubMed: 16493418]

Thiery JP, Acloque H, Huang RY, Nieto MA. Epithelial-mesenchymal transitions in development and disease. Cell. 2009; 139:871–890. [PubMed: 19945376]

Toedling J, Skylar O, Krueger T, Fischer JJ, Sperling S, Huber W. Ringo—an R/Bioconductor package for analyzing ChIP-chip readouts. BMC Bioinformatics. 2007; 8:221. [PubMed: 17594472]

Van Rechem C, Black JC, Abbas T, Allen A, Rinehart CA, Yuan GC, Dutta A, Whetstine JR. The SKP1-Cul1-F-box and leucine-rich repeat protein 4 (SCF-FbxL4) ubiquitin ligase regulates lysine demethylase 4A (KDM4A)/Jumonji domain-containing 2A (JMJD2A) protein. J. Biol. Chem. 2011; 286:30462–30470. [PubMed: 21757720]

Vega S, Morales AV, Ocañ a OH, Valdés F, Fabregat I, Nieto MA. Snail blocks the cell cycle and confers resistance to cell death. Genes Dev. 2004; 18:1131–1143. [PubMed: 15155580]

Wagner JM, Hackanson B, Lübbert M, Jung M. Histone deacetylase (HDAC) inhibitors in recent clinical trials for cancer therapy. Clin. Epigenetics. 2010; 1:117–136. [PubMed: 21258646]

Wu MZ, Tsai YP, Yang MH, Huang CH, Chang SY, Chang CC, Teng SC, Wu KJ. Interplay between HDAC3 and WDR5 is essential for hypoxia-induced epithelial-mesenchymal transition. Mol. Cell. 2011; 43:811–822. [PubMed: 21884981]

Yang J, Weinberg RA. Epithelial-mesenchymal transition: at the crossroads of development and tumor metastasis. Dev. Cell. 2008; 14:818–829. [PubMed: 18539112]

Yu M, Smolen GA, Zhang J, Wittner B, Schott BJ, Brachtel E, Ramaswamy S, Maheswaran S, Haber DA. A developmentally regulated inducer of EMT, LBX1, contributes to breast cancer progression. Genes Dev. 2009; 23:1737–1742. [PubMed: 19651985]

Zeitlinger J, Zinzen RP, Stark A, Kellis M, Zhang H, Young RA, Levine M. Whole-genome ChIP-chip analysis of Dorsal, Twist, and Snail suggests integration of diverse patterning processes in the Drosophila embryo. Genes Dev. 2007; 21:385–390. [PubMed: 17322397]

Zhang J, Smolen GA, Haber DA. Negative regulation of YAP by LATS1 underscores evolutionary conservation of the Drosophila Hippo pathway. Cancer Res. 2008; 68:2789–2794. [PubMed: 18413746]

Zhou BP, Deng J, Xia W, Xu J, Li YM, Gunduz M, Hung MC. Dual regulation of Snail by GSK-3beta-mediated phosphorylation in control of epithelial-mesenchymal transition. Nat. Cell Biol. 2004; 6:931–940. [PubMed: 15448698]

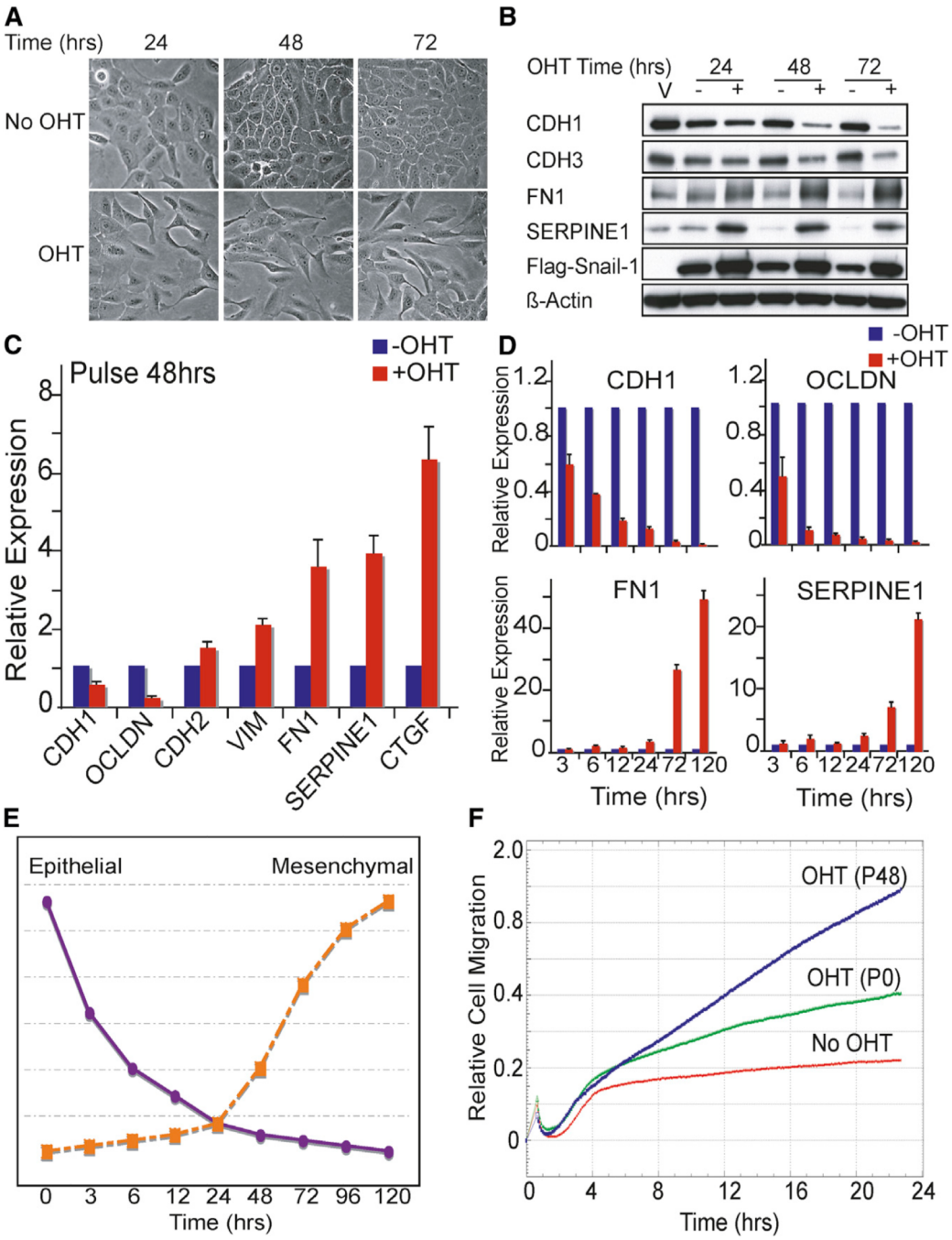

Figure 1. Expression of Epithelial and Mesenchymal Genes in Response to Snail-1 Induction

(A) Light-microscopic images of MCF10A cells infected with ER-Snail-1^{S6A} following exposure to 4-OHT for 24, 48, and 72 hr.

(B) Immunoblot of epithelial (CDH1 and CDH3) and mesenchymal (FN1 and SERPINE1) markers in response to 4-OHT treatment of ER-Snail-1^{S6A}-transduced cells. β-actin serves as loading control. V denotes parental noninfected MCF10A cells.

(C) mRNA expression (qRT-PCR) of epithelial (CDH1 and OCLDN) and mesenchymal (CDH2, VIM, FN1, SERPINE1, and CTGF) genes 48 hr after 4-OHT-mediated induction of Snail-1. Error bars represent SEM.

(D) mRNA expression (qRT-PCR) of epithelial (CDH1 and OCLDN) and mesenchymal (FN1 and SERPINE1) genes following 3, 6, 12, 24, 72, and 120 hr of 4-OHT. Error bars represent SEM.

(E) Mean trendline of epithelial (CDH1 and OCLDN) and mesenchymal (FN1 and SERPINE1) gene expression following Snail-1 expression.

(F) Real-time cell migration (Roche xCElligence system) of Snail-1 transduced MCF10A cells in the absence of 4-OHT (No OHT), upon 4-OHT exposure at 0 hr (P0), and after 48 hr of pretreatment with 4-OHT (P48).

See also Figure S1.

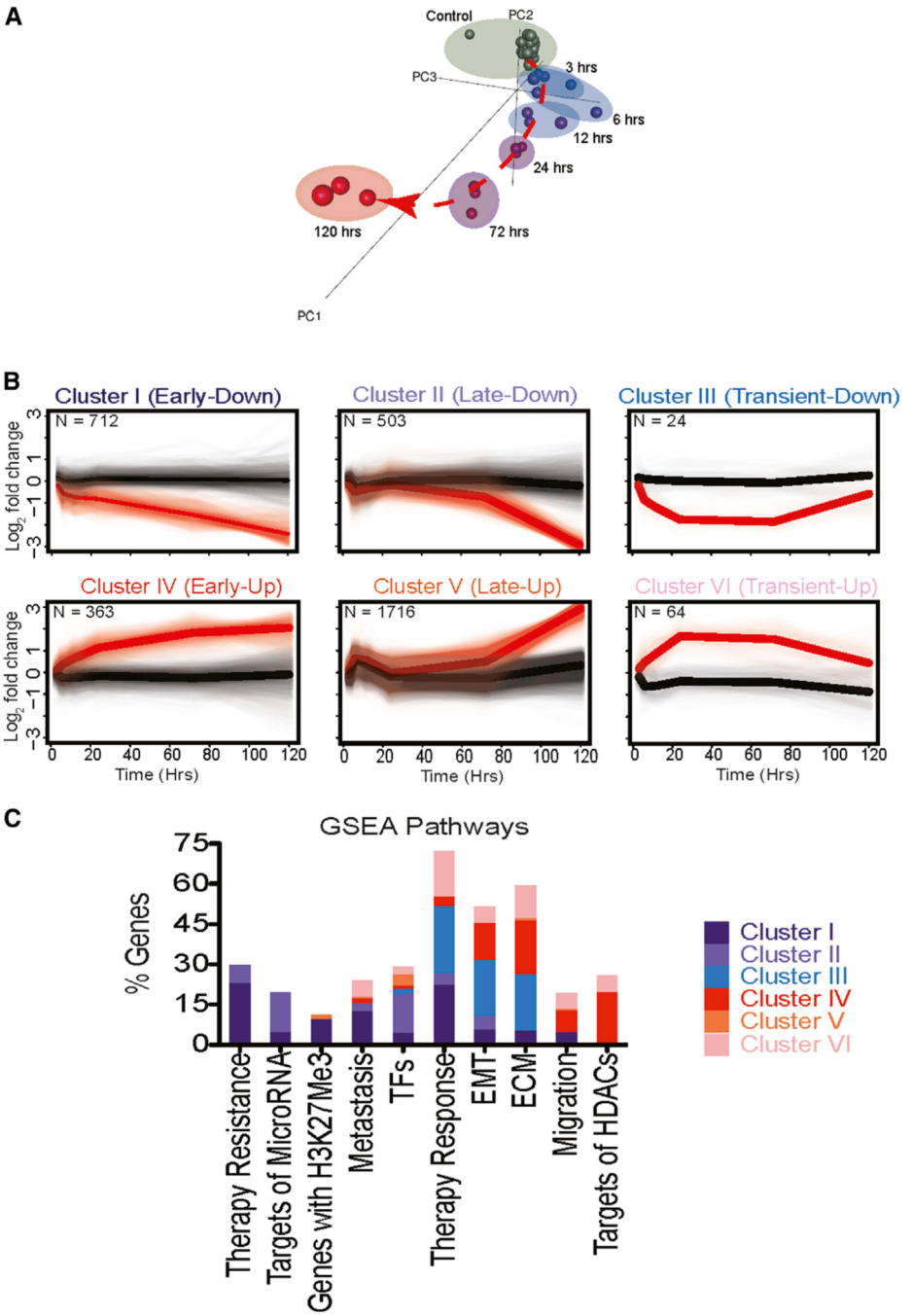

Figure 2. Dynamic Gene-Expression Patterns Associated with Acute Induction of EMT

(A) PCA plot of microarray-based expression profiling for MCF10A Snail-1-induced cells (time points: 3, 6, 12, 24, 72, and 120 hr; each time point is normalized to its respective control (untreated) time point).

(B) Clusters I–III represent early-, late-, and transiently repressed genes, respectively. Clusters IV–VI are early-, late-, and transiently induced genes, respectively. Black and red lines represent untreated and Snail-1-induced MCF10A cells, respectively.

(C) GSEA-derived pathways identified as enriched within individual gene-expression clusters through a gene set signature. Individual GSEA gene signatures and classifications are shown in Tables S1–S6.

See also Table S7.

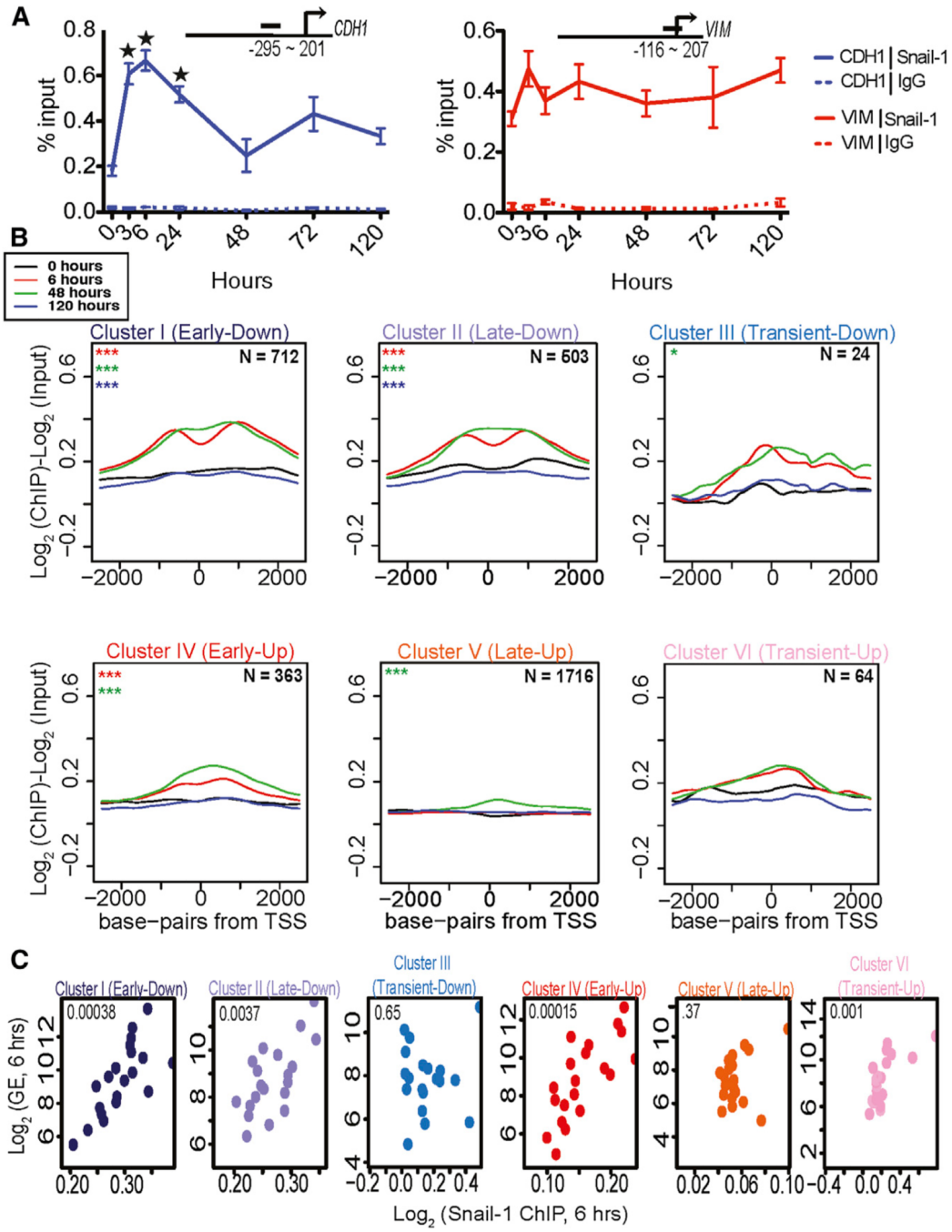

Figure 3. Transient Binding of Snail-1 to Its Target Promoters

(A) ChIP-qPCR analysis of Snail-1 versus IgG control at the CDH1 and VIM promoters at 0, 3, 6, 24, 48, 72, and 120 hr after addition of 4-OHT. *p%0.001. Error bars represent SEM.

(B) ChIP-chip $\log_2$ ratio of Snail-1 immunoprecipitation at 0, 6, 48, and 120 hr after 4-OHT addition. Promoter sequences span from −2 kb to +2 kb of TSS, and these are shown for early-, late-, and transiently repressed genes (clusters I–III) and early-, late-, and transiently induced genes (clusters IV–VI). *p % 0.05, **p % 0.01, and ***p % 0.001. Red, green, and blue colors represent 6, 48, and 120 hr compared with the 0 hr time point, respectively.

(C) Correlation between Snail-1 promoter binding and specific gene expression at the 6 hr time point. Genes were sorted into 20 equal-size bins based on expression levels (log_2 GE), with the average of Snail-1 ChIP-chip (log_2 ChIP) intensity at promoters and expression levels shown for each bin. The Spearman p value is shown within each cluster (Nie et al., 2012).

See also Figure S2 and Table S8.

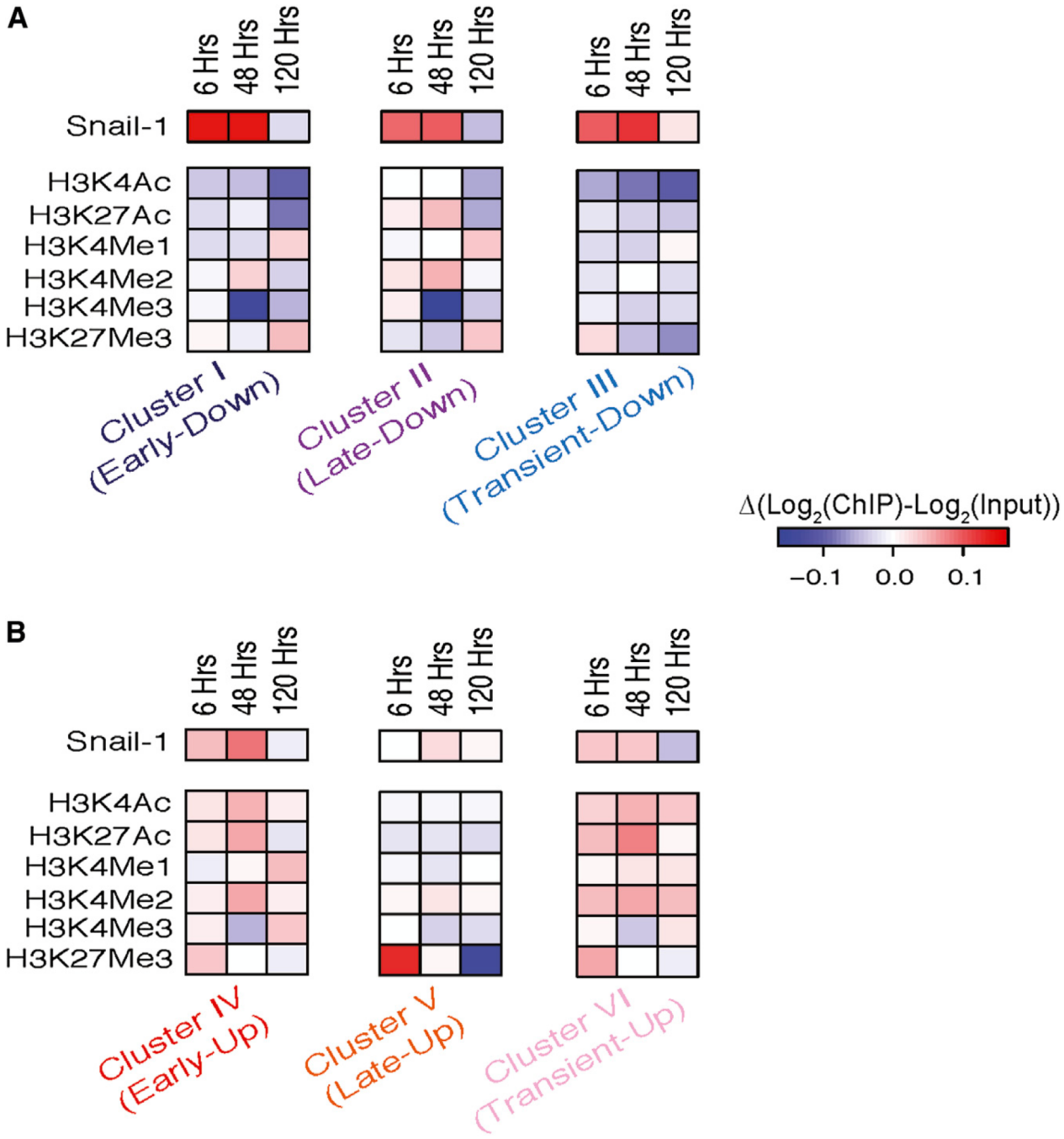

Figure 4. Transient and Sustained Snail-1-Induced Chromatin Marks Associated with Gene-Expression Clusters

(A and B) ChIP-chip $\log_2$ heatmap of Snail-1, H3K4Ac, H3K27Ac, H3K4Me1, H3K4Me2, H3K4Me3, and H3K27Me3 immunoprecipitates at 6, 48, and 120 hr compared with 0 hr after Snail-1 induction. Heatmap results are shown for −2 kb to +2 kb promoter regions of genes whose expression is altered by Snail-1: early- (cluster I), late- (cluster II), and transiently (cluster III) repressed transcripts; and early- (cluster IV), late- (cluster V), and transiently (cluster VI) induced transcripts.

See also Figures S3 and S4.

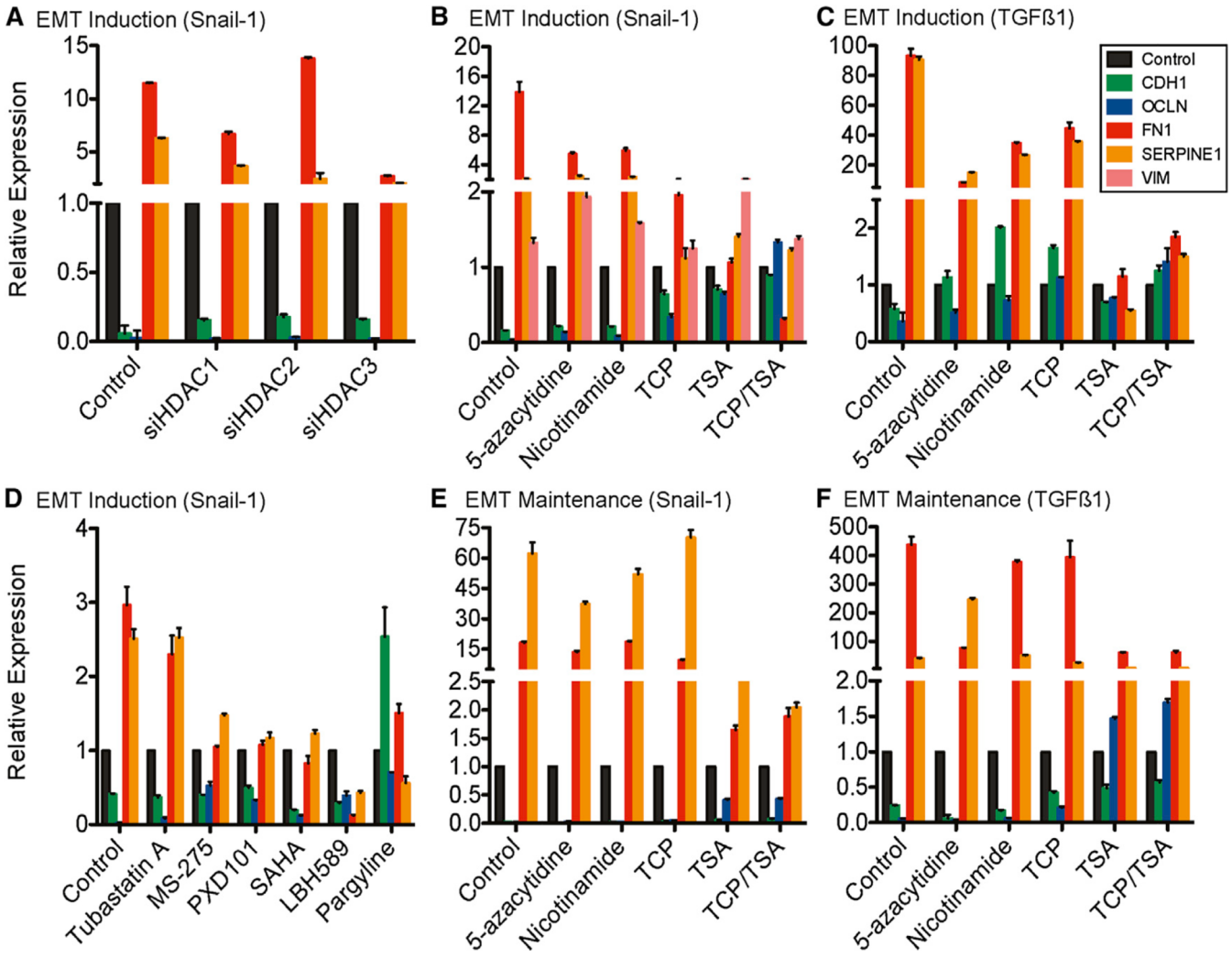

Figure 5. Suppression of EMT by Small-Molecule Inhibitors of Chromatin Regulators

(A) Changes in expression of epithelial (CDH1 and OCLDN) and mesenchymal (FN1 and SERPINE1) genes 48 hr after Snail-1 induction in cells with RNAi knockdown of HDAC1, HDAC2, or HDAC3. siRNA transfection was performed 24 hr prior to 4-OHT addition (see data in Figure S5A). Error bars represent SEM.

(B) Epithelial and mesenchymal gene expression induced by Snail-1 following treatment of cells with small-molecule inhibitors of chromatin regulators. Drugs were added to cells 24 hr prior to 4-OHT treatment and maintained for another 48 hr. Error bars represent SEM.

(C) Effect of small-molecule inhibitors of chromatin regulators on TGF-β-induced (48 hr) EMT. Drugs were added 24 hr before initiation of treatment with TGF-β. Error bars represent SEM.

(D) Effect of selective small-molecule inhibitors on Snail-1-mediated EMT. Drugs were added to cells 24 hr prior to 4-OHT treatment and maintained for another 48 hr. Error bars represent SEM.

(E) Reversibility of established Snail-1-induced EMT (6 days with 4-OHT) by treatment of cells with small-molecule inhibitors for 24 hr. Error bars represent SEM.

(F) Reversibility of established TGF-β-induced EMT (12 days with TGF-β) following 24 hr treatment with inhibitors. Error bars represent SEM.
See also Figures S5 and S6.

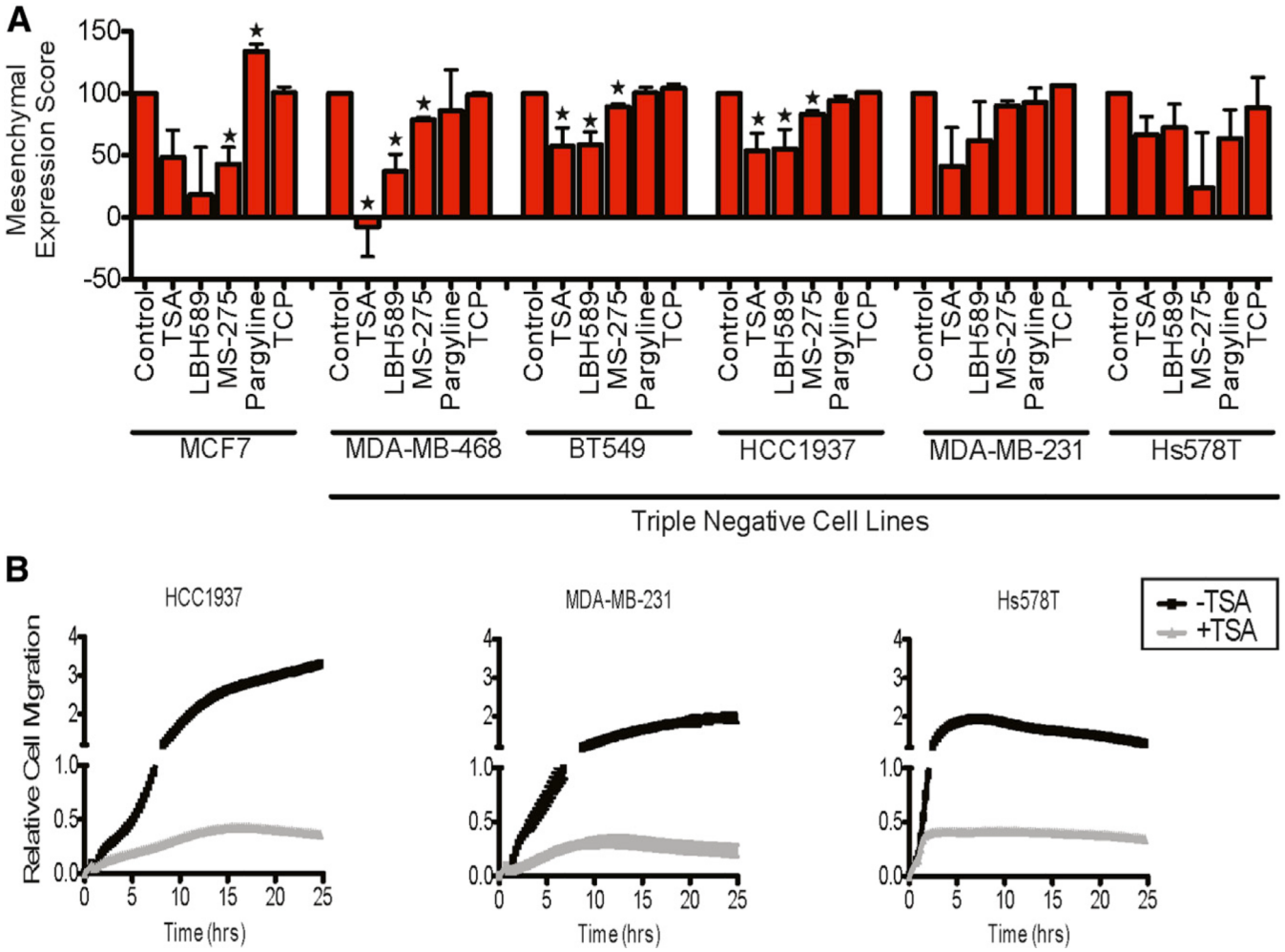

Figure 6. Suppression of Mesenchymal Markers and Migration by Small-Molecule Inhibitors in Triple-Negative Cancer Lines

(A) Reversibility of mesenchymal markers in established cancer cell lines (triple-negative breast cancer) following treatment with small-molecule inhibitors for 24 hr. Expression of mesenchymal (FN1, SERPINE1, and VIM) genes were assayed (Fluidigm qRT-PCR) at 24 hr. *p%0.05. Student's t test for mean of mesenchymal gene markers, for each drug-treated cell line compared with control DMSO-treated cell line (data in Figures S6B and S6C).

(B) Real-time cell migration (Roche xCElligence system) of HCC1937, MDA-MB-231, and Hs578T following treatment (24 hr) with and without TSA. Migration of BT549 and MDA-MB-468 is not shown because there was minimal effect.

See also Figure S6.